Sensor and Simulation Notes

Note 328

24 June 1991

Aperture Efficiencies for IRAs

Carl E. Baum

Phillips Laboratory

Abstract

This paper considers the characteristics of the aperture shape and size for launching the impulsive portion of approximate impulse-radiating-antenna (IRA) waveforms. Using complex-variable techniques the electric field on the aperture plane (early time) is assumed to have the distribution of a TEM plane wave (inhomogeneous) on the aperture and is formulated as a complex field given by the derivative of the complex potential with respect to the complex coordinate (two dimensional). The surface integral is converted to a contour integral around the aperture for ease in evaluation. This is used to define appropriate characteristic lengths for the aperture which can be maximized for best impulsive operation. The aperture optimization is applied to both TEM horns and TEM-fed reflectors, which are shown to have complementary structures on the aperture plane.

Sensor and Simulation Notes

Note 328

24 June 1991

Aperture Efficiencies for IRAs

Carl E. Baum

Phillips Laboratory

Abstract

This paper considers the characteristics of the aperture shape and size for launching the impulsive portion of approximate impulse-radiating-antenna (IRA) waveforms. Using complex-variable techniques the electric field on the aperture plane (early time) is assumed to have the distribution of a TEM plane wave (inhomogeneous) on the aperture and is formulated as a complex field given by the derivative of the complex potential with respect to the complex coordinate (two dimensional). The surface integral is converted to a contour integral around the aperture for ease in evaluation. This is used to define appropriate characteristic lengths for the aperture which can be maximized for best impulsive operation. The aperture optimization is applied to both TEM horns and TEM-fed reflectors, which are shown to have complementary structures on the aperture plane.

impulse radiating antenna (IRA), TEM waves, plane waves

I. Introduction

In a previous paper [4] it was shown that a step-rising tangential electric field on an aperture S_a in a plane S gives a delta-function-like field in the far field for an observer as $r \to \infty$ along a direction perpendicular to the aperture. This is a plane-wave illuminated aperture which can be extended to directions of propagation at arbitrary angles with respect to the aperture plane. This is not an exact delta function due to the problem of transition from near to far field in time domain since s (complex frequency) covers frequencies extending to infinity. However, the area under the pulse (time integral) is well described by the impulse (delta-function) formulas. Furthermore, practical antennas fed by finite-energy pulsers alter the aperture illumination to give a low-frequency limitation so that the total pulse has undershoot to give a net zero area. See [4] for a discussion of these limitations and the form the pulse takes off the main beam (plane-wave aperture illumination direction).

As indicated in fig. 1.1 let there be an aperture S_a in the x, y plane denoted S. As developed in [4] the far field is

$$\tilde{\bar{E}}_f(\vec{r},s) = \frac{s\, e^{-\gamma r}}{2\pi c r}\left[\left(\vec{1}_z \cdot \vec{1}_r\right)\bar{1} - \vec{1}_z\vec{1}_r\right] \cdot \int_{S_a} e^{\gamma \vec{1}_r \cdot \vec{r}'}\, \tilde{\bar{E}}_t(\vec{r}',s)\, dS'$$

$c = \left[\mu_o \epsilon_o\right]^{-1/2}$ = speed of light

s ≡ Laplace-transform variable

$= \Omega + j\omega$ ≡ complex frequency

$\gamma \equiv \frac{s}{c}$ ≡ free space propagation constant

~ ≡ Laplace transform (two-sided) over time

$\vec{1}_r \equiv \frac{\vec{r}}{r}$, $\vec{r} = (x,y,z)$

$\bar{1} \equiv \vec{1}_x\,\vec{1}_x + \vec{1}_y\,\vec{1}_y + \vec{1}_z\,\vec{1}_z$ ≡ dyadic identity (1.1)

Specialize to an aperture distribution as

$$\vec{E}_t(\vec{r}',s) = e^{-\gamma \vec{1}_o \cdot \vec{r}'} E_o\, \tilde{f}(s)\, \vec{g}(\vec{r}')$$

$\tilde{f}(s)$ ≡ waveform on aperture

$\vec{g}(\vec{r}')$ ≡ aperture spatial distribution

$\vec{1}_o$ ≡ direction of propagation of plane-wave aperture distribution

= focal direction in far field (1.2)

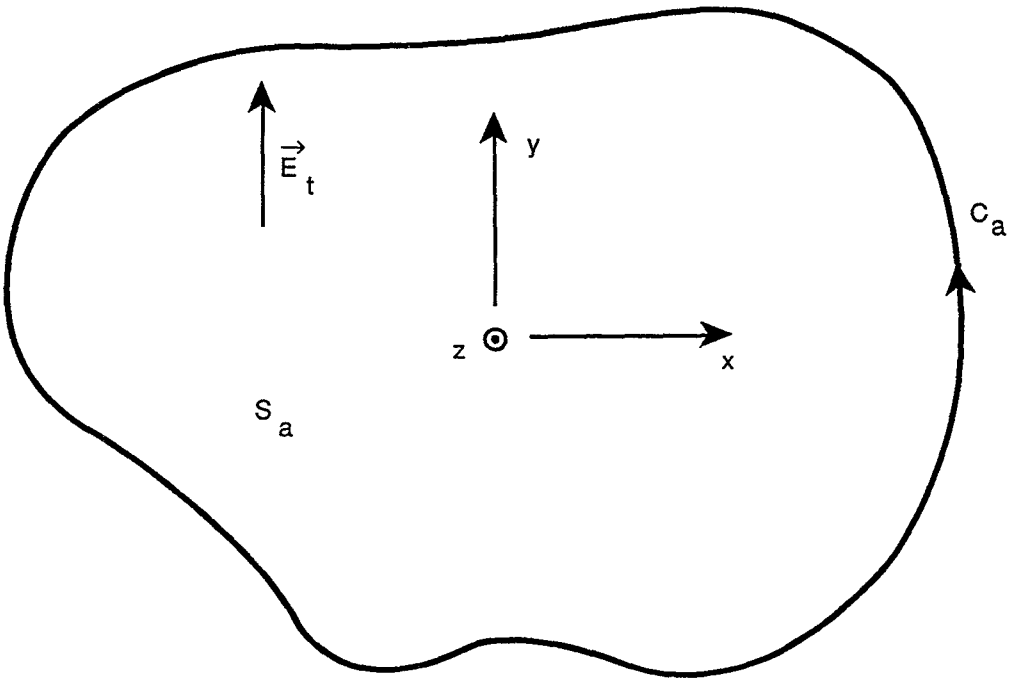

Fig. 1.1. Aperture with Specified Tangential Electric Field

This gives

$$\vec{\tilde{E}}_f(\vec{r},s) = e^{-\gamma r}\ \frac{E_o A}{2\pi c r}\ \vec{\tilde{F}}\left(\vec{1}_r,s\right)$$

$A \equiv$ aperture area

$$\vec{\tilde{F}}\left(\vec{1}_r,s\right) \equiv s\tilde{f}(s)\ \vec{\tilde{F}}_a\left(\vec{1}_r,s\right) \equiv \text{far-field waveform function}$$

$$\vec{\tilde{F}}_a\left(\vec{1}_r,s\right) \equiv \frac{1}{A}\left[\left(\vec{1}_z\cdot\vec{1}_r\right)\vec{1}-\vec{1}_z\vec{1}_r\right]\cdot\int_{S_a} e^{\gamma\left[\vec{1}_r-\vec{1}_o\right]\cdot\vec{r}'}\,\vec{g}(\vec{r}')\ dS'$$

$\equiv$ aperture function (1.3)

This can be evaluated for various waveforms and directions $\vec{1}_r$ both on and off the focal direction $\vec{1}_o$ in both frequency and time. An interesting special case is for ideal step-function illumination

$$\tilde{f}(s) = \frac{1}{s}$$

$$\vec{\tilde{F}}\left(\vec{1}_r,s\right) \equiv \vec{\tilde{F}}_a\left(\vec{1}_r,s\right) \tag{1.4}$$

so that the far-field time-domain waveform is just $\vec{F}_a\left(\vec{1}_r,t\right)$. Letting the observer be on the focal direction we have

$$\vec{1}_r = \vec{1}_o$$

$$\vec{F}_a\left(\vec{1}_r,t\right) \equiv \frac{\delta(t)}{A}\left[\left(\vec{1}_z\cdot\vec{1}_r\right)\vec{1}-\vec{1}_z\vec{1}_r\right]\cdot\int_{S_a}\vec{g}(\vec{r}')\ d\vec{r}' \tag{1.5}$$

which is the ideal result of a δ function radiator. Again note that as discussed in [4], the correct field is limited in amplitude by the aperture field with a small pulse width to give the correct impulse (or time integral) as above. Note for the special case of boresight (normal to aperture)

$$\vec{1}_r = \vec{1}_o = \vec{1}_z$$

$$\vec{F}_a\left(\vec{1}_r,t\right) \equiv \frac{\delta(t)}{A}\int_{S_a}\vec{g}(\vec{r}')\ d\vec{r}'$$

$$\vec{E}_f(\vec{r},t) \equiv \frac{E_o}{2\pi c r}\ \delta(t)\int_{S_a}\vec{g}(\vec{r}')\ d\vec{r}' \tag{1.6}$$

Formally we can define a modified delta function appropriate to the aperture in question with

$$\int_{-\infty}^{\infty} \delta_a(r,t)\ dt = 1 \qquad (1.7)$$

where δ_a is a function of r as well as t, its peak being proportional to r and width proportional to r^{-1}. This makes δ_a/r have a peak which is constant with r (appropriate to large r) so that the peak field at early retarded times is constant for the simple cases discussed in [4]. This $\delta_a(r, t)$ can be substituted for $\delta(t)$ in (1.6) and calculated for specific cases if desired.

II. Vector Size of Aperture Under TEM Illumination.

Now specify our aperture fields as

$$\vec{E}_t(\vec{r}',t) = \vec{E}(x',y')\ u(t) \tag{2.1}$$

giving the ideal far field as

$$\vec{E}_f(\vec{r},t) = \frac{\delta(t)}{2\pi cr} \oint_{S_a} \vec{E}(x',y')\ dS' \tag{2.2}$$

(with use of δ_a if desired). In order to define some effectiveness for the aperture as an impulse radiator we need something related to the surface integral above.

Note that $\vec{E}_f \cdot \vec{E}_f/Z_o$ is a power density in the far field. Assuming a TEM-like field $\vec{E}(x,y)\ u(t)$ on the aperture (at least for early times) gives a power fed into the antenna by integrating all such power including that which does not illuminate the aperture. So let us define

$$A_\delta \equiv \frac{\frac{1}{Z_o}\left|\int_{S_a} \vec{E}(x,y)\ dS\right|^2}{P_{in}}$$

$$Z_o = \left[\frac{\mu_o}{\epsilon_o}\right]^{\frac{1}{2}} \equiv \text{wave impedance of free space} \tag{2.3}$$

where P_{in} is the power fed into the antenna immediately following the step rise. This gives some effective area as can be seen by checking the units. More conveniently define

$$\vec{a}_\delta \equiv \frac{\int_{S_a} \vec{E}(x,y)\ dS}{[Z_o\ P_{in}]^{1/2}}$$

$$A_\delta = \vec{a}_\delta \cdot \vec{a}_\delta \tag{2.4}$$

Thus $\vec{a}_\delta$ contains polarization information and is some effective length of the aperture, the far field impulse (for just this part of the waveform) scaling with this parameter. One could have used voltage or current feeding the antenna for normalization, but an ideal transformer can scale these up or down arbitrarily. Thus power seems more appropriate.

Now assume that the aperture is fed by the TEM mode of a cylindrical transmission line, an inhomogeneous TEM plane wave, the wave propagating parallel to the z axis, and hence perpendicular to S. As a practical matter this is a long conical transmission line, sufficiently long that the fields arrive essentially simultaneously on S_a, the time-of-arrival differences being smaller than all other times of interest. Alternately, as discussed in [4], this conical transmission line can be shortened by use of a lens or parabolic reflector to change the spherical TEM wave into a plane wave, with the TEM property at least approximately retained.

Now let the fields on S be characterized by a TEM mode as on a two-conductor (perfectly conducting) cylindrical transmission line in free space. As discussed in Appendix A this is characterized by voltage V and current I (after step rise) with

$$\frac{V}{I} = Z_c = f_g \; Z_o \equiv \text{characteristic impedance}$$

$$f_g = \frac{\Delta u}{\Delta v} \equiv \text{geometrical impedance factor}$$

$$P_{in} = V\,I = \frac{V^2}{Z_c} \tag{2.5}$$

Substituting these in (2.4) gives

$$\vec{a}_\delta \equiv \frac{\sqrt{f_g}}{V} \int_{S_a} \vec{E}(x,y)\; dS \tag{2.6}$$

Going further let (as in Appendix B)

$$\zeta = x + jy \equiv \text{complex coordinate}$$

$$w(\zeta) = u + jv \equiv \text{complex potential} \tag{2.7}$$

The electric field (tangential) is the gradient of a scalar potential as

$$\vec{E}(x,y) = E_x \vec{1}_x + E_y \vec{1}_y = -\nabla\Phi(x,y) = -\frac{V}{\Delta u}\; \vec{e}_o(x,y)$$

$$\vec{e}_o(x,y) = \nabla u(x,y) \tag{2.8}$$

This can also be set in complex form as

$$E(\zeta) = E_x - jEy = -\frac{V}{\Delta u}\; \frac{dw(\zeta)}{d\zeta} \tag{2.9}$$

Now rewrite $\vec{a}_\delta$ in complex form via

$$\vec{a}_\delta = a_{\delta_x} \vec{1}_x + a_{\delta_y} \vec{1}_y$$

$$a_\delta = a_{\delta_x} - j a_{\delta_y}$$

$$A_\delta = \vec{a}_\delta \cdot \vec{a}_\delta = |\vec{a}_\delta|^2 = a_\delta \; a_\delta^* = |a_\delta|^2 \tag{2.10}$$

Then (2.6) becomes

$$a_\delta = -[\Delta u\ \Delta v]^{-1/2} \int_{S_a} \frac{dw}{d\zeta} dS$$

$\Delta u \equiv$ change in u between the two conductors

$\Delta v \equiv$ change in v in going around either conductor (noting not to cross branch cut) (2.11)

As we can now see a_δ is a function of w and the aperture S_a, basically a function of the TEM transmission line and aperture geometries.

As shown in Appendix B the surface integral can be replaced by a contour integral around C_a, the aperture boundary, giving various forms as

$$a_\zeta = -[\Delta u\ \Delta v]^{-1/2} \frac{j}{2} \oint_{C_a} w\, d\,\zeta^* = -f_g^{\frac{1}{2}} \frac{j}{2\Delta v} \oint_{C_a} w d\zeta^*$$

$$= -[\Delta u\ \Delta v]^{-1/2}\ j \oint_{C_a} u d\zeta^* = -f_g^{\frac{1}{2}} \frac{j}{2\Delta v} \oint_{C_a} u d\zeta^*$$

$$= [\Delta u\ \Delta v]^{-1/2} \oint_{C_a} v d\zeta^* = f_g^{\frac{1}{2}} \frac{1}{\Delta v} \oint_{C_a} v d\zeta^* \quad (2.12)$$

See (B.6) through (B.9) for various other forms including those using dx and dy separately as well. Note that C_a should not cross branch cuts, but this is easily avoided by breaking up S_a with C_a as a set of contours around the pieces.

We are now in a position to compare various antenna designs via a_δ. This can be converted to an efficiency, if desired, by dividing by some linear dimension of the antenna, e.g. maximum linear dimension, cube root of the volume, etc.

An interesting question concerns the maximization of $|a_\delta|$ by appropriate choice of S_a (and hence C_a). Appendix D shows how to evaluate a_δ for the case that S_a is extended to all S via S_∞ (radius $\Psi_\infty \to \infty$) as

$$a_{\delta_\infty} = -f_g^{-1/2}\,\frac{1}{\Delta v}\int_{S_\infty}\frac{dw}{d\zeta}\,dx\,dy$$

$$= -jf_g^{-1/2}\,\frac{1}{\Delta v}\oint_{C_\infty} u\,d\zeta^* = f_g^{-1/2}\,\frac{1}{\Delta v}\oint_{C_\infty} v\,d\zeta^*$$

$$= -f_g^{-1/2}\,\frac{h_e}{2}$$

$h_e \equiv h_{e_x} - jh_{e_y} \equiv$ equivalent height

$\equiv$ mean charge separation distance between two conductors (2.13)

where C_∞ is deformed as necessary to exclude branches.

Also in Appendix C it is shown that other shapes of aperture with size$\to\infty$ give different answers. In particular one can increase $|a_\delta|$ above that in (2.13). One may ask how big $|a_\delta|$ might be made by appropriate choice of the shape of S_a for a given h_e. For this purpose let us define another length for the aperture

$$h_a \equiv h_{a_x} - jh_{a_y} \equiv -f_g^{1/2}a\zeta$$

$$= \frac{1}{\Delta v}\int_{S_a}\frac{dw}{d\zeta}\,dxdy = \frac{j}{\Delta v}\oint_{C_a} u\,d\zeta^* = -\frac{1}{\Delta v}\oint_{C_a} v\,d\zeta^* \qquad (2.14)$$

and compare this for various aperture choices. As we have already seen

$$\frac{h_a}{h_e} = \begin{cases} 1/2 \text{ for } S_\infty \text{ aperture (Appendix D)} \\ 1 \text{ for } S_v \text{ aperture (Appendix D)} \end{cases} \qquad (2.15)$$

where the S_v aperture corresponds to using constant v contours with $v = v_o \to 0$ (filling up the plane) for two wires in Appendix D.

Now S_a does not have to be infinite. Various shapes can be investigated for application to antenna design. An example in Appendix C2 is for a circular aperture of diameter $|h_e|$ with wires feeding two diametrically opposite parts of the aperture, right on the edge of the aperture. There it is shown that

$$h_a = \frac{h_e}{2} \qquad (2.16)$$

which is the same as for the S_∞ aperture.

In order to increase $|a_\delta|$, and hence $|h_e|$, one can decide which portions of S to use. Define some particular direction, say $\vec{i}_a$, as the direction of the principal field (tangential electric field on the aperture) of

interest. For cases of sufficient symmetry in the TEM feed and S_a this is an obvious direction antiparallel to $\vec{h}_e$. Looking at the field on S_a, then wherever it is parallel to $\vec{1}_a$ (positive dot product) this field will contribute positively to the surface integral as in (2.2), so this region can be chosen as part of S_a.

A simple but practical case of this has

$$\vec{1}_a = -\vec{1}_y$$

$$\vec{h}_a = h_{a_y}\ \vec{1}_y \quad , \quad h_a = -jh_{a_y} \quad , \quad h_{a_y} < 0$$

$$\vec{h}_e = h_{e_y}\ \vec{1}_y \quad , \quad h_e = -jh_{e_y} \quad , \quad h_{e_y} > 0 \tag{2.17}$$

so that the principal field is in the -y direction. Assume that the x, z and y, z planes are planes of symmetry for both the TEM conductors and S_a to assure the resultant y components as above, as well as the reduction of the integration to a single quadrant of the ζ plane.

From (2.14) we now have for our symmetric case

$$h_{a_y} = -f_g^{1/2}\ a_{\delta_y} = -\frac{1}{\Delta v}\oint_{C_a} u\,dx = -\frac{1}{\Delta v}\oint_{C_a} v\,dy$$

$$= -\frac{4}{\Delta v}\oint_{C'_a} u\,dx = -\frac{4}{\Delta v}\oint_{C'_a} v\,dy \tag{2.18}$$

where C'_a is the positive contour around S'_a, that portion of S_a in the upper right or first quadrant of the ζ plane. See an example in fig. C.2. Note that C'_a strictly does not include the conductor cross sections (the field here being zero anyway). This form using C'_a makes it easy to avoid crossing branch cuts.

A simple case has $u = 0$ on the x axis so that we can write

$$h_{a_y} = \frac{4}{\Delta v}\int_0^{x_{max}} u_a\ dx_a$$

x_{max} ≡ maximum extent of S'_a in +x direction

u_a ≡ electric potential along C'_a portion excluding x and y axes (2.19)

Thinking of u_a as the integral from $y = 0$ up to C'_a along a constant x of the negative of the electric field, then (2.19) completes the integration over x. Note that if C'_a includes portions of the y axis both above and below the upper conductor this formula is still appropriate, the integral along C'_a around the conductor boundary giving zero due to the constant u there. Implicitly u_a in (2.19) has been taken as single valued (i.e. C'_a having only one y for each x away from the two axes). This is not a restriction in that (2.19) can easily be modified to allow for such a case. Similarly the formula involving the magnetic potential v in (2.18) can be cast into an appropriate integral over y analogous to (2.19).

Appendix C evaluates (2.19) for various aperture shapes for a symmetrical two-wire TEM aperture feed with equivalent line charges on the y axis at $\pm b_e$ on the edge of the aperture. Comparing to the circular aperture in (2.16) we have

$$\frac{h_{a_y}}{h_{e_y}} = \begin{cases} .5 & \text{circular aperture} \\ 1 & \text{strip aperture (rectangular, infinitely wide)} \\ .55 & \text{square aperture} \\ \to \infty & \text{hyperbolic upper and lower y aperture boundaries (infinitely wide) maximizing integrand in (2.19)} \end{cases}$$

$$h_{e_y} = 2b_e \tag{2.20}$$

III. Complementary Field Suppressors and Reflectors with TEM Transmission-Line Feeds

With the discussion in Section II we can now see that there is a certain complementary relationship on the aperture plane between TEM horns and TEM fed reflectors. The aperture S_a is chosen so that the locations on S with positive contributions to the integral for h_a (electric field with a component in the same direction as the principal field, $-\vec{h}_e$) are included in S_a and other locations are excluded.

For an ideal TEM horn (infinitely long cylindrical TEM transmission line) as in fig. 3.1A, the portions excluded from S_a are covered with field suppressing (perfectly conducting) sheets. Conversely for the ideal reflector in fig. 3.1B (planar with infinitely long TEM transmission line) S_a is covered with field reflecting (perfectly conducting) sheets. The aperture S_a can be chosen the same for both except for practical considerations of finite size for the conductors.

Practically and desirably the TEM waveguides can be conical so as to have finite length, say ℓ, from the aperture plane. As illustrated in fig. 3.2A, the equivalent height is appropriately (for present analysis) the spacing h of the conductors (charge centers) at the aperture plane. The length ℓ is chosen so that the dispersion distance d [2]

$$d = \left[\ell^2 + \Psi_a^2\right]^{1/2} - \ell \simeq \frac{\Psi_a^2}{2\ell} \tag{3.1}$$

is small compared to both ℓ and Ψ_a (the largest radius of S_a of interest) and is small enough that d/c is a sufficiently short time that negligible broadening of the impulsive part of the radiated field occurs. Alternatively a nondistorting transient lens [12] is placed just before the aperture plane to convert the spherical TEM wave into a planar one at the aperture plane. The lens, of course, allows ℓ to be significantly decreased while still having negligible dispersion time (time difference of arrival on the aperture plane). Note the inclusion of field-suppressing conductors as discussed previously.

Consider now the TEM-fed reflector as in fig. 3.2B. In principle this can be planar, but with the same restriction on large ℓ for small dispersion distance (over the entire reflector). Now the effect of the aperture blockage due to the conical TEM conductors should be considered. In the high-frequency limit the blockage can be reduced by appropriate choice of the shape of the TEM conductors [5]. This may also influence the choice of f_g since a small value (low impedance) implies fat conductors which increase the aperture blockage. In terms of a_δ the aperture blockage can be considered as a reduction in S_a with relevant portions being deleted from the integral. Note that the field reflected from S_a is the negative of the incident field. Of course the reflector is best not a plane, but a paraboloid, allowing a significant reduction in ℓ for the reflected field to be a plane wave on an aperture plane just in front of the reflector. The paraboloidal reflector serves the same function as a lens.

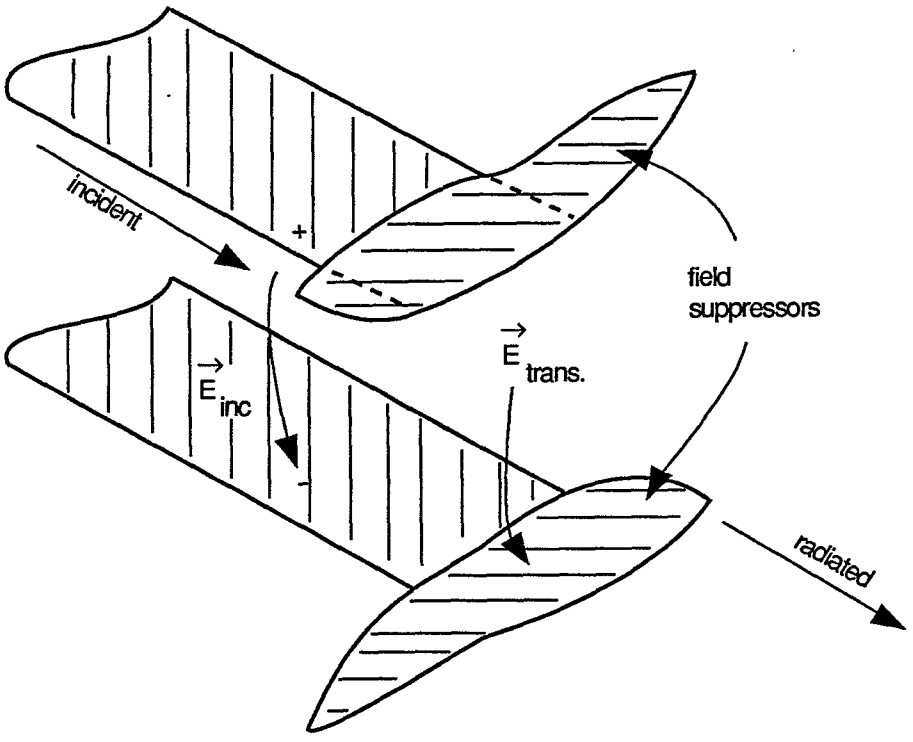

A. Ideal cylindrical transmission line with
suppressor sheets for undesired aperture fields

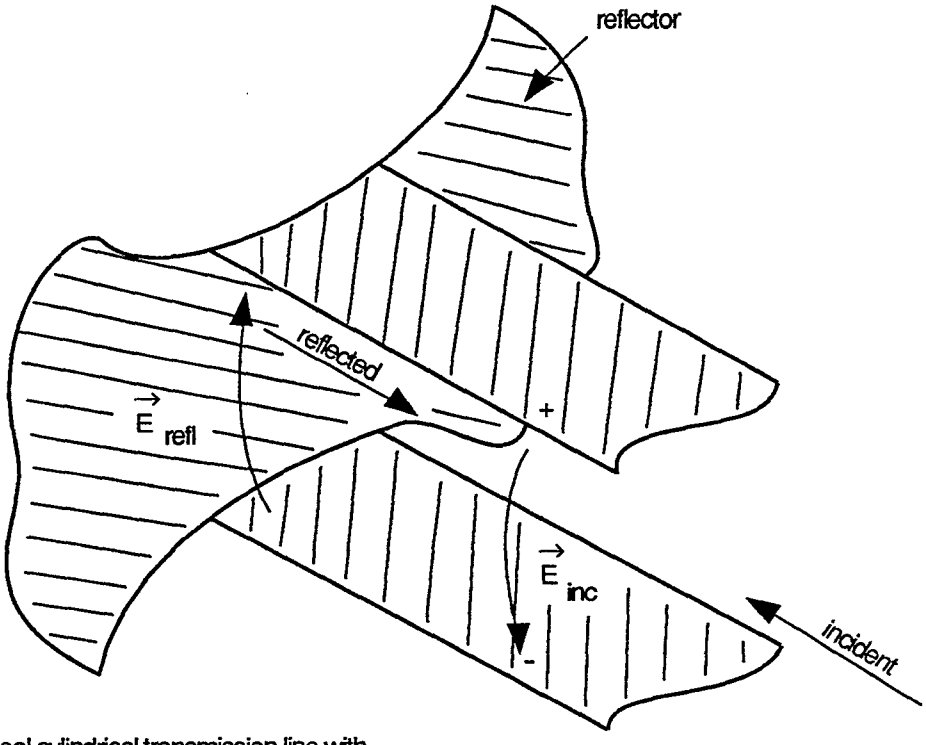

B. Ideal cylindrical transmission line with
reflector sheet for desired aperture fields

Fig. 3.1. Complementary Relationship of TEM Horns and TEM-Fed Reflectors

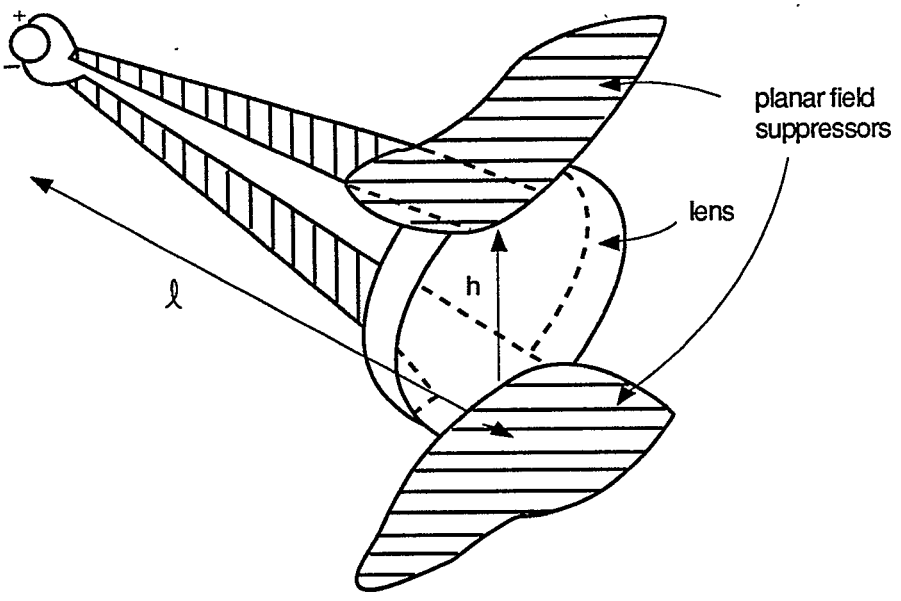

A. TEM horn, possibly with lens

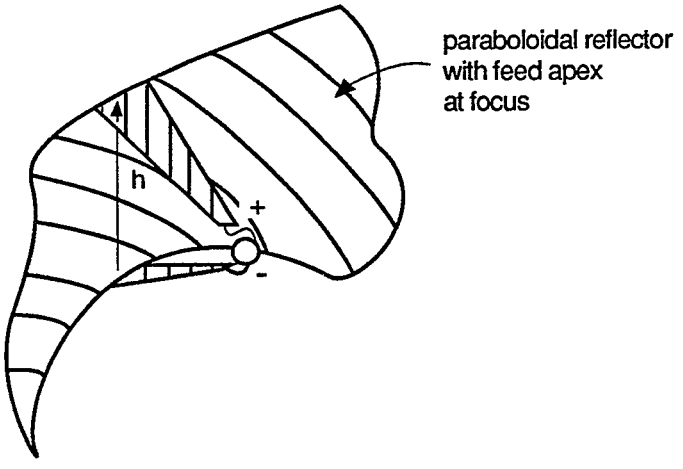

B. TEM fed reflector

Fig. 3.2. Practical Forms of TEM-Fed Apertures

IV. Finite-Length TEM Horns

Some further insight into the performance of an IRA for the impulsive part of the waveform can be gained by looking at the early-time radiation from finite-length TEM horns. As indicated in fig. 3.2A let the conical apex be placed behind the aperture plane ($z = 0$ plane) a distance ℓ with a step-rising voltage $V\,u(t + \ell/c)$. Let the TEM horn be composed of flat-sheet cones with a spacing h at the aperture plane (equivalent height there). Then let the plate dimensions at the aperture plane be

$$2a \equiv \text{width}$$

$$2b = h \equiv \text{separation} \tag{4.1}$$

One can roughly approximate the early field on the aperture (E_y) by $-V_o/h$ with arrival time based on the spherical wavefront ($t = 0$ being arrival in the center of the aperture) [6]. For a distant observer on the $+z$ axis the spherical wave can be extrapolated for early time as

$$\vec{E}_f \simeq -\frac{V}{2a}\,\frac{\ell}{r}\,\vec{1}_y \tag{4.2}$$

The width t_o of this early pulse can be written as

$$c\,t_o = \left[\ell^2 + \Psi_o^2\right]^{\frac{1}{2}} - \ell = \frac{\Psi_o^2}{2\ell} \text{ as } \frac{\Psi_o}{\ell} \to 0 \tag{4.3}$$

where Ψ_o is some effective radius of the aperture related to the time that the spherical wave arrives at the plate intersection with the aperture. One might make a crude estimate for Ψ_o as a or $\sqrt{a^2 + b^2}$. The impulse or area under the radiated waveform is

$$\vec{E}_f\,t_o = -\frac{V}{4cr}\,\frac{\Psi_o^2}{a}\,\vec{1}_y \text{ as } \frac{\Psi_o}{\ell} \to 0 \tag{4.3}$$

Note for small Ψ_o / ℓ that this is independent of ℓ. The pulse amplitude in (4.2) and the pulse width in (4.3) depend on ℓ, but not this impulse.

The impulse in (4.3) depends on Ψ_o^2/a a characteristic dimension of the aperture, since for a given aperture shape Ψ_o/a is a dimensionless constant. This says that the impulse depends on the linear dimensions of the aperture, and is proportional to h (or a or Ψ_o). So to first order it is the aperture size and not ℓ (the length of the feeding conical transmission line) which is important for the impulse.

Compare this formula for the impulse to the one for a plane-wave illuminated aperture in (2.2), (2.6), and (2.14) as

$$\int_{-\infty}^{0+} \vec{E}_f(\vec{r},t)dt = \frac{1}{2\pi cr} \int_{S_a} \vec{E}(x',y')\ dS'$$

$$= \frac{1}{2\pi cr}\ V\ f_g^{-\frac{1}{2}}\ \vec{a}_\delta$$

$$= -\frac{1}{2\pi cr}\ V\ \vec{h}_a = -\frac{1}{2\pi cr}\ V\ h_{a_y}\ \vec{1}_y \qquad (4.4)$$

Noting the common factors we have

$$h_{a_y} = \frac{\pi}{2}\frac{\Psi_o^2}{a}\ ,\quad \Psi_o = \left[\frac{2}{\pi}\ a\ h_{a_y}\right]^{\frac{1}{2}} \qquad (4.5)$$

where h_{a_y} has been defined in terms of an integral over the aperture. This can be considered to define Ψ_o (the effective radius of the aperture). Substituting back in (4.3) then gives the effective width of the radiated impulse for the TEM horn.

V. Concluding Remarks

Here the behavior of the impulsive part of an IRA waveform has been characterized in terms of the integral of the tangential electric field on the aperture, ideally a step function turning on at $t = 0$, simultaneously over the entire aperture. This has been converted to normalized forms as characteristic dimensions of the aperture a_δ and h_a, the latter closely related to the equivalent height of the TEM transmission-line feed, while the former also includes the geometric factor in the feeding TEM-transmission-line impedance.

The analysis here applies to both TEM horns (perhaps with lenses) and TEM-fed reflectors. Best performance (narrow impulse) is obtained by a fast rising pulse on the aperture with a simultaneity of arrival (plane wave) to a time shorter than the rise time. To accomplish this, a TEM horn can be made very long, or a lens included near the aperture. A paraboloidal reflector can efficiently accomplish the same purpose. With these considerations in mind, one can design a short feed with a large aperture, noting that the radiated impulse is proportional to the aperture size. Depending on the design details the aperture fields will approximate a TEM field distribution to various degrees. A more exact analysis may take this into account.

There is a complementary relationship between the TEM horn and TEM-fed aperture on the aperture plane. In designing an optimum aperture S_a one wishes to utilize portions of S (the aperture plane) that contribute to the relevant integrals by having a field component in the direction of the principal electric field. (Symmetry helps here.) Then for the TEM horn, field suppressing conducting sheets can be placed on portions of S not included in the optimum S_a, while for the TEM-fed reflector the reflector is placed on portions of the optimum S_a.

One can carry this concept further by using other than perfectly conducting sheets for reflectors and field suppressors. Uniconducting sheets (constructed as grids of (locally) parallel closely spaced wires) can be used to reflect or transmit desired components of the fields incident on the aperture plane. While this can be used to increase the contribution to the surface integral of the tangential electric field, the increase may not be great, particularly when compared to the increased difficulty of construction and other parasitic effects (e.g. resonances on the grid).

This paper has considered the impulsive part of the IRA waveform. There are various other portions of interest as discussed in [4]. These are affected by various features of the antenna design, including the design of the feed, terminations, and pulser. These affect the lower frequency portions of the response including pattern, as a general broadband radiator [5]. While our attention here has been focused on the high-frequency performance in the center of the beam, off center characteristics are also of interest as in [4]. In addition sidelobes (say due to the feed spillover past the reflector) need to be considered and perhaps suppressed by strategic placement of absorbing materials, perhaps in the region of S outside S_a where the fields are still large.

Appendix A. Complex Potentials and Fields for Two-Dimensional TEM-Mode Description

For TEM modes propagating in the z direction we have the complex coordinate and potential as [2]

$$\zeta \equiv x + jy$$

$$w(\zeta) = u(\zeta) + jv(\zeta) \tag{A.1}$$

With w an analytic function of ζ (appropriate to solutions of the Laplace equation in two dimensions) we have the Cauchy-Riemann conditions

$$\frac{\partial u}{\partial x} = \frac{\partial v}{\partial y} \quad , \quad \frac{\partial u}{\partial y} = -\frac{\partial v}{\partial x} \tag{A.2}$$

In terms of vector fields we have electric and magnetic normalized fields

$$\vec{e}_o(x,y) \equiv \nabla u(x,y) \quad , \quad \vec{h}_o(x,y) \equiv \nabla v(x,y)$$

$$\vec{W}(x,y) \equiv \nabla w(x,y) \tag{A.3}$$

In complex form we have

$$e_o(\zeta) = e_{o_x}(x,y) - je_{o_y}(x,y) \quad , \quad h_o(\zeta) = h_{o_x}(x,y) - jh_{o_y}(x,y)$$

$$e_{o_x}(x,y) = h_{o_y}(x,y) \quad , \quad e_{o_y}(x,y) = -h_{o_x}(x,y)$$

$$e_o(\zeta) = jh_o(\zeta) = \frac{dw(\zeta)}{d\zeta} \tag{A.4}$$

Given two conductors (assumed perfect) with cross sections for constant z as indicated in fig. A.1, we have potentials on the two conductors with

$$V = \Phi_+ - \Phi_- \quad , \quad \Delta u = u_+ - u_-$$

$$\Phi(x,y) = \frac{V}{\Delta u}\, u(x,y)$$

$$\vec{E}(x,y) = -\nabla\Phi(x,y) = -\frac{V}{\Delta u}\, \vec{e}_o(x,y) \tag{A.5}$$

Similarly we have a magnetic potential with

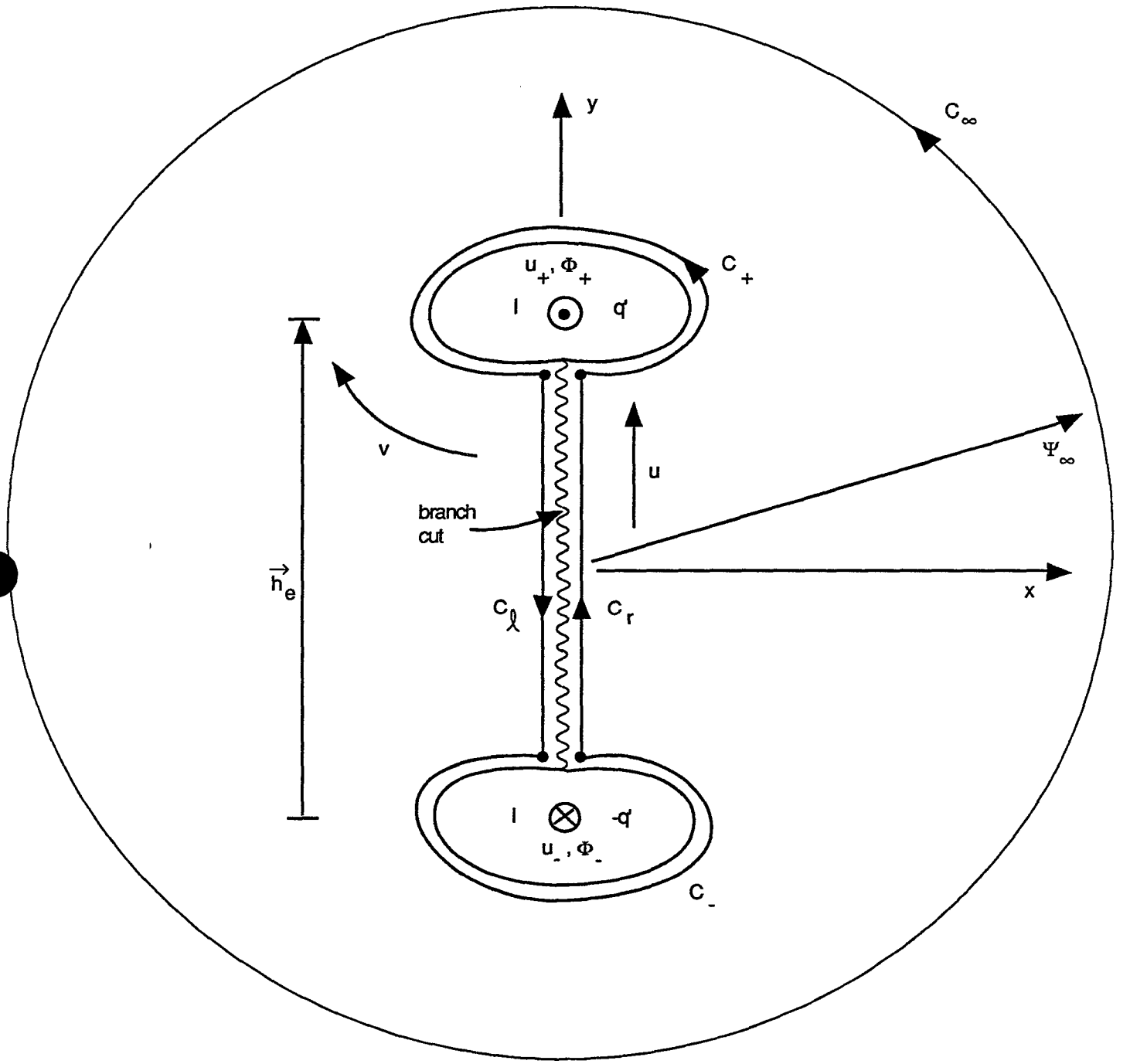

$$C_o = C_+ \cup C_\ell \cup C_- \cup C_r$$

Fig. A.1. Two Conductors with Zero Net Charge Per Unit Length and Current

$$I = \Phi_m \oint_{C_-} = -\Phi_m \oint_{C_+} , \quad \Delta v = v \oint_{C_-} = -v \oint_{C_+}$$

$$\Phi_m(x,y) = \frac{I}{\Delta v}\, v(x,y)$$

$$\vec{H}(x,y) = -\nabla \Phi_m(x,y) = -\frac{I}{\Delta v}\, \vec{h}_o(x,y) \tag{A.6}$$

Here the change in the functions Φ_m and v around the contour is taken in the positive sense as indicated in fig. A.1. We have taken the "upper" conductor as positive with current out of the page (+2). There is a branch cut connecting the two conductors so that v can be defined in a single-valued way. Note that C_+ and C- do not cross this cut, but approach it arbitrarily close on both sides. These end points are used to define the change around the contours as in (A.6). Alternately one could define the branch cut as two branch cuts, one running from each conductor to infinity. In terms of these parameters we have, assuming the medium is free space,

$$f_g \equiv \frac{\Delta u}{\Delta v} \equiv \text{geometrical impedance factor}$$

$$Z_c = f_g\, Z = \frac{V}{I} \equiv \text{characteristic impedance}$$

$$Z = \left[\frac{\mu_o}{\epsilon_o}\right]^{\frac{1}{2}} = \text{wave impedance} \tag{A.7}$$

$$L' = \mu_o\, f_g \equiv \text{inductance per unit length}$$

$$C' = \frac{\epsilon_o}{f_g} \equiv \text{capacitance per unit length}$$

$$c = \left[\mu_o\, \epsilon_o\right]^{-1/2} = \left[L'\, C'\right]^{-1/2} \equiv \text{speed of light}$$

In our present class of problems we assume that the net current and charge per unit length on the conductors are zero, i.e.

$$q' = q'_+ = -q'_- \quad , \quad I = I_+ = -I_- \tag{A.8}$$

This allows $w(\zeta)$ to be single valued in going around the set of conductors on both

C_∞ $\left(\text{on } |\zeta| = \Psi_\infty \to \infty\right)$ and

$$C_o = C_+ \cup C_\ell \cup C_- \cup C_r \tag{A.9}$$

Note the inclusion of C_r and C_ℓ (with indicated orientations) on both sides of the branch cut.

Note that vector fields (transverse to z) can now be replaced by complex fields as

$$E(\zeta) = -\frac{V}{\Delta u}\,\frac{dw(\zeta)}{d\zeta} = -\frac{V}{\Delta u}\,e_o(\zeta) = E_x - jE_y$$

$$H(\zeta) = -\frac{I}{\Delta v}\,h_o(\zeta) = -j\frac{I}{\Delta v}\,e_o(\zeta) = H_x - jH_y$$

$$\frac{E(\zeta)}{H(\zeta)} = j\frac{V}{I}\,\frac{\Delta v}{\Delta u} = j\frac{Z_c}{f_g} = j\,Z_o \qquad \text{(A.10)}$$

Appendix B. Surface Integral of TEM Fields in a Plane

A fundamental quantity of interest is the integral of the tangential electric field over the aperture

$$\vec{Y} = Y_x \vec{i}_x + Y_y \vec{i}_y = \int_{S_a} \vec{E}(x,y)dS = \int_{S_a} \vec{E}(x,y)dxdy \tag{B.1}$$

with units Vm here. Using the complex field (Appendix A) we have

$$Y = Y_x - jY_y = \int_{S_a} \vec{E}(\zeta)dxdy = \int_{S_a} \left[E_x - jE_y\right]dxdy$$

$$= -\frac{V}{\Delta u}\int_{S_a} e_o dxdy = -\frac{V}{\Delta u}\int_{S_a} \frac{dw(\zeta)}{d\zeta}\,dxdy \tag{B.2}$$

Our problem is then reduced to evaluating

$$W_a \equiv W_x - jW_y = \int_{S_a} \frac{dw(\zeta)}{d\zeta}\,dxdy \tag{B.3}$$

Note first that we have [7]

$$\frac{dw(\zeta)}{d\zeta} = \frac{\partial w}{\partial x} = \frac{\partial u}{\partial x} + j\frac{\partial v}{\partial x}$$

$$= j\frac{\partial w}{\partial y} = \frac{\partial v}{\partial w} - j\frac{\partial u}{\partial y} \tag{B.4}$$

as expressions for the complex derivative which can be used with the Cauchy-Riemann conditions in (A.2). Next we use Green's theorem on a plane [11] which says that for Ψ_1 and Ψ_2 continuously differentiable on S

$$\int_{S_a} \frac{\partial \psi_1}{\partial x}\,dxdy = \oint_{C_a} \psi_1 dy$$

$$-\int_{S_a} \frac{\partial \psi_2}{\partial y}\,dxdy = \oint_{C_a} \psi_2 dx$$

$$\int_{S_a}\left[\frac{\partial \psi_1}{\partial x} - \frac{\partial \psi_2}{\partial y}\right]dxdy = \oint_{C_a}\left[\psi_1 dy + \psi_2 dx\right] \tag{B.5}$$

with C_a the positive contour around S_a. Multiply connected regions are also allowed, e.g. the region between C_∞ (outside) and C_o (inside) by interpreting C_a as $C_\infty \cup (-C_o)$, noting now the negative orientation of C_o.

Applying the various form of (B.5) to (B.3) we find for C_a enclosing S_a

$$W = \int_{S_a} \frac{dw}{d\zeta}\, dxdy = \int_{S_a} \frac{\partial w}{\partial x}\, dxdy = \oint_{C_a} w dy$$

$$= -j \int_{S_a} \frac{\partial w}{\partial y}\, dxdy = j \oint_{C_a} w dx \tag{B.6}$$

Combining these we have

$$W = \int_{S_a} \frac{dw}{d\zeta}\, dxdy = \frac{1}{2} \oint_{C_a} w[jdx + dy]$$

$$= \frac{j}{2} \oint_{C_a} w d\zeta^* \tag{B.7}$$

Compare this to the Cauchy theorem for w analytic in S_a

$$\oint_{C_a} w d\zeta = 0 \tag{B.8}$$

which is consistent since (B.7) has the conjugate $d\zeta^*$. Other forms in terms of u and v are

$$\mathrm{Re}[W_a] = \int_{S_a} \frac{\partial u}{\partial x} dxdy = \int_{S_a} \frac{\partial v}{\partial y} dxdy$$

$$= \oint_{C_a} u dy = -\oint_{C_a} v dx$$

$$\mathrm{Im}[W_a] = -\int_{S_a} \frac{\partial u}{\partial y} dxdy = \int_{S_a} \frac{\partial v}{\partial x} dxdy$$

$$= \oint_{C_a} u dx = \oint_{C_a} v dy$$

$$W = j \oint_{C_a} u d\zeta^* = -\oint_{C_a} v d\zeta^* \tag{B.9}$$

These results are a kind of Stoke's theorem applied to analytic functions in the complex plane.

Some supporting results are found by special choice of w as

$$\oint_C d\zeta = 0 \tag{B.10}$$

which implies

$$\oint_C dx = 0 \ , \oint_C dy = 0 \ , \oint_C d\zeta^* = 0 \tag{B.11}$$

Appendix C. Symmetrical Two-Wire Transmission Line as Antenna Feed

To illustrate some of the concepts let us consider a two-wire cylindrical transmission line for the TEM mode to use in our calculations [1]. Let these wires of radius a be centered at y=±b on the y,z plane (x = 0). The z = 0 plane is taken as the aperture plane. (See fig. C.1.)

1. General formulas

As in (A.5) we have

$$\Phi = \frac{V}{\Delta u}\, u = \frac{q'}{C'}\,\frac{u}{\Delta u} = \frac{q'}{C' f_g}\,\frac{u}{\Delta u} = \frac{q'}{\epsilon_o}\,\frac{u}{\Delta v}$$

$$w = \ell n\left[\frac{\frac{\zeta}{b_e}+j}{\frac{\zeta}{b_e}-j}\right] = 2\text{jarccot}\left(\frac{\zeta}{b_e}\right)$$

$$\Delta v = 2\pi \tag{C.1}$$

Now as discussed in [1] the equivalent charge (or current) position is

$$b_e = \left[b^2 - a^2\right]^{\frac{1}{2}} \tag{C.2}$$

The separate potentials are

$$u = \frac{1}{2}\,\ell n\left[\frac{\left(\frac{x}{b_e}\right)^2 + \left(1+\frac{y}{b_e}\right)^2}{\left(\frac{x}{b_e}\right)^2 + \left(1-\frac{y}{b_e}\right)^2}\right]$$

$$v = \arctan\left[\frac{2\frac{x}{b_e}}{\left(\frac{x}{b_e}\right)^2 + \left(\frac{y}{b_e}\right)^2 - 1}\right] \tag{C.3}$$

On the conductors we have

$$u_+ = -u_- = \text{arccosh}\left(\frac{b}{a}\right) = \ell n\left[\frac{b}{a} + \left(\left(\frac{b}{a}\right)^2 - 1\right)^{\frac{1}{2}}\right]$$

$$\Delta u = 2u_+ = -2u_- \tag{C.4}$$

giving

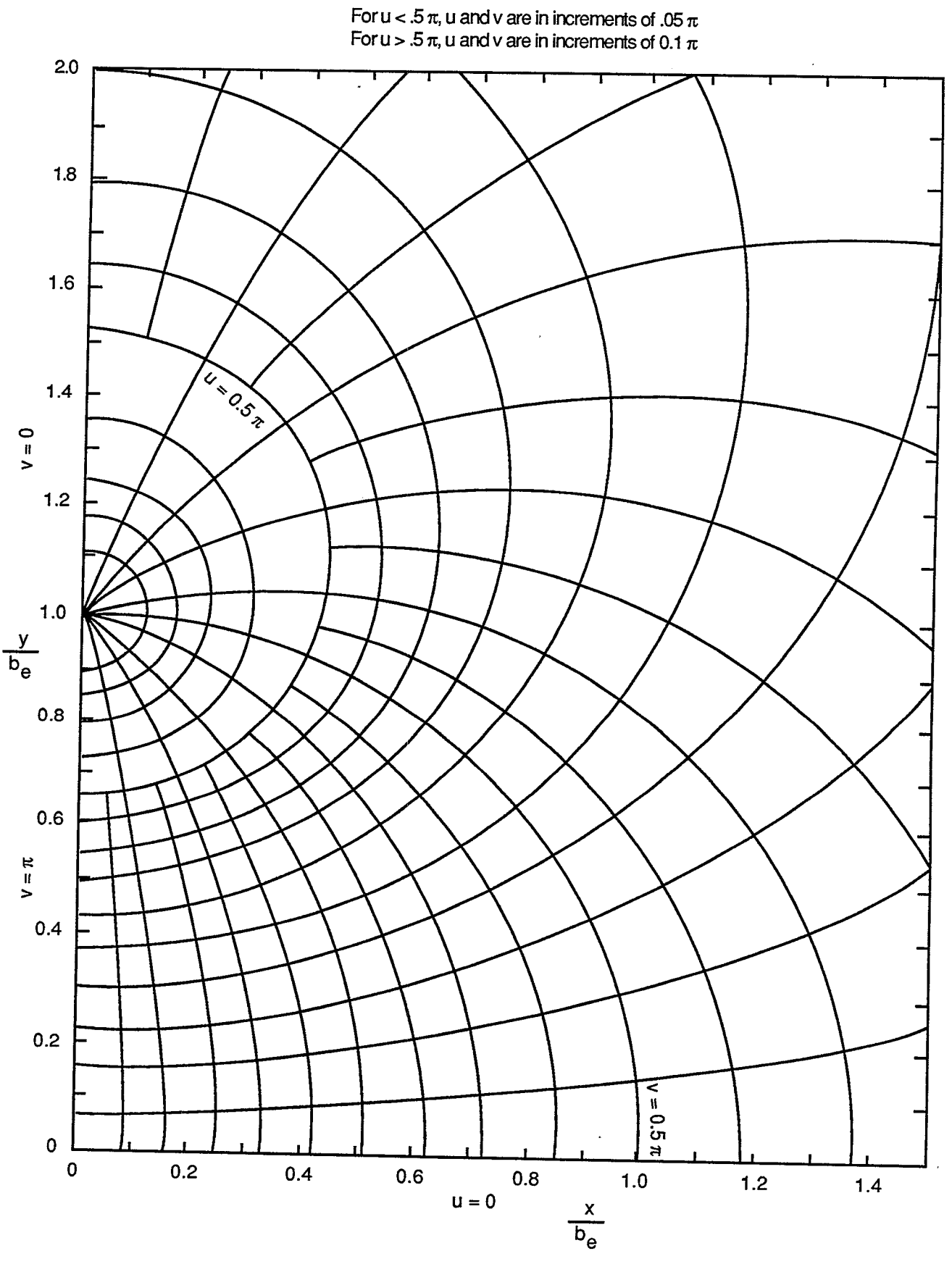

Figure C.1. Potential Distribution for Symmetrical Two-Wire Transmission Line

$$f_g = \frac{\Delta u}{\Delta v} = \frac{1}{\pi}\, \ell n \left[\frac{b}{a} + \left(\left(\frac{b}{a}\right)^2 - 1 \right)^{\frac{1}{2}} \right]$$

$$= \frac{1}{\pi}\, \ell n \left[\frac{b + b_e}{a} \right]$$

$$= \frac{1}{\pi} \text{ arccosh} \left(\frac{b}{a} \right)$$

$$= \frac{1}{\pi} \text{ arcsinh} \left(\frac{b_e}{a} \right) \qquad \text{(C.5)}$$

From (2.11, (2.12) and (B.6) through (B.9) the aperture effective length is

$$a_\delta = - \left[\Delta u \ \Delta v \right]^{-\frac{1}{2}} W_a$$

$$W_a = j \oint_{C_a} u d\zeta^* = - \oint_{C_a} v d\zeta^* \qquad \text{(C.6)}$$

Here restricting S_a to be symmetric with respect to the y axis we have only a y component for the surface integral of the field as in (2.6) and hence only an imaginary component of a_δ as

$$a_\delta = - j a_{\delta_y}$$

$$a_\delta = [\Delta u \Delta v]^{-1/2} \oint_{C_a} u dx = [\Delta u \Delta v]^{-1/2} \oint_{C_a} v dy$$

$$= f_g^{-1/2} \ \frac{1}{2\pi} \oint_{C_a} u dx = f_g^{-1/2} \ \frac{1}{2\pi} \oint_{C_a} v dy \qquad \text{(C.7)}$$

Referring to fig. C.2 now let the aperture be symmetric with respect to both x and y axes. Using the contour integration results in Appendix B, the contour integral over C_a can be replaced by a set of contour integrals around separate parts of the aperture S_a. The contour integrals should not cross branch cuts, or more specifically u or v as required in (C.6) and (C.7) have to be single valued over the aperture or appropriate portions thereof. Then with both wires of radius a centered on the y axis at $\pm$b we can consider one quadrant (x>0, y>0) of the ζ plane. Call this subaperture S'_a with contour C'_a as indicated. Then we have precisely one quarter of the aperture integral from S'_a for a_{δ_y} giving

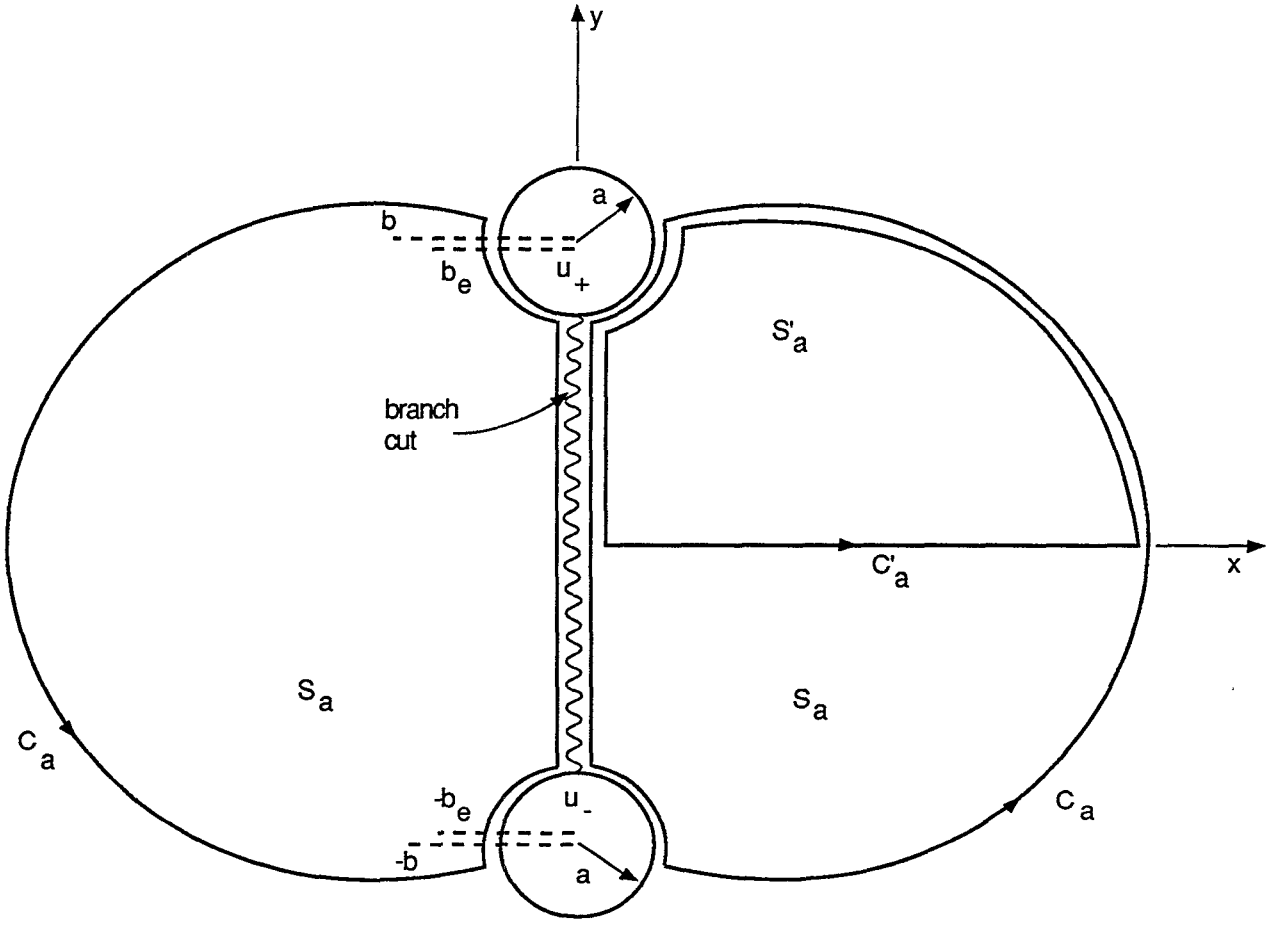

Fig. C.2. Aperture Integration for Symmetrical Two-Wire Transmission Line

$$a_{\delta_y} = 4[\Delta u \Delta v]^{-1/2} \oint_{C'_a} u dx = 4[\Delta u \Delta v]^{-1/2} \oint_{C'_a} v dy$$

$$= f_g^{-1/2} \frac{2}{\pi} \oint_{C'_a} u dx = f_g^{-1/2} \frac{2}{\pi} \oint_{C'_a} v dy \qquad \text{(C.8)}$$

For convenience another parameter h_a from Section II here is

$$h_a = h_{a_x} - j h_{a_y}$$

$$h_{a_y} = -f_g^{1/2} a_{\delta_y} = -\frac{2}{\pi} \oint_{C'_a} u dx = -\frac{2}{\pi} \oint_{C'_a} v dy \qquad \text{(C.9)}$$

As will be seen this is closely related to the equivalent height h_e where for the present problem

$$h_e = -j h_{e_y} \ , \ h_{e_y} = 2 b_e \qquad \text{(C.10)}$$

2. S_a bounded by circular arcs of constant v

First consider the inverse of the transformation in (C.1), i.e. [1]

$$\frac{\zeta}{b_e} = \cot\left(-\frac{j}{2} w\right) = j \coth\left(\frac{w}{2}\right)$$

$$\frac{x}{b_e} = \frac{\sin(v)}{\cosh(u) - \cos(v)}$$

$$\frac{y}{b_e} = \frac{\sinh(u)}{\cosh(u) - \cos(v)} \qquad \text{(C.11)}$$

Curves of constant u (electric equipotentials) are circular given by

$$\left(\frac{x}{b_e}\right)^2 + \left[\frac{y}{b_e} - \coth(u)\right]^2 = \operatorname{csch}^2(u) \qquad \text{(C.12)}$$

Similarly curves of constant v (magnetic equipotentials) are also circles, but given by

$$\left[\frac{x}{b_e} - 2\cot(v)\right]^2 + \left(\frac{y}{b_e}\right)^2 = \csc^2(u) \qquad \text{(C.13)}$$

and passing through the equivalent line charge on the y axis at $\pm b_e$.

So now let C'_a have its upper right portion a curve of constant v-v_o. Note that for large f_g the upper conductor has a circular contour of small radius a. The integral over v (between v_o and π) on the conductor portion of C'_a is small. So using

$$h_{a_y} = -\frac{2}{\pi}\oint_{C'_a} v\,dy \tag{C.14}$$

we have for small a

$$h_{a_y} = \frac{2}{\pi}[\pi - v_o]\; b_e \left[1 + 0\left(\frac{a}{b}\right)\right] \text{ as } \frac{a}{b} \to 0 \tag{C.15}$$

the value of v on the y axis (between the conductors) being π (limit from the right). An interesting special case has a contour

$$v_o = \frac{\pi}{2}\,,\; x^2 + y^2 = b_e^2 \text{ (circular disk } S_a) \tag{C.16}$$

For such a circular aperture we have

$$h_{a_y} = b_e \left[1 + 0\left(\frac{a}{b}\right)\right] \text{ as } \frac{a}{b} \to 0 \tag{C.17}$$

Letting $v_o \to 0$ then S'_a fills the upper right quadrant of the ζ plane (excluding the wire) and we have

$$h_{a_y} = 2b_e \left[1 + 0\left(\frac{a}{b}\right)\right] \text{ as } \frac{a}{b} \to 0 \tag{C.18}$$

i.e. twice as much as for the circular aperture of radius b_e. Stated another way the circular aperture is half as efficient in contributing to the surface integral of the tangential electric field as the entire plane S, provided S is defined by the limit as $v_o \to 0$.

3. S_a including all of S_∞

For the case that S_a covers all of S in the sense of S_∞ (i.e. of radius $\Psi_\infty \to \infty$) we have from Appendix D

$$a\delta_{y_\infty} = -\frac{1}{2}\, f_g^{-1/2}\, h_{e_y} = -f_g^{-1/2}\; b_e = -a\left(\left(\frac{b}{a}\right)^2 - 1\right)^{1/2} \left[\frac{1}{\pi}\,\text{arccosh}\left(\frac{b}{a}\right)\right]^{-1/2} \tag{C.19}$$

We can ask from this what is a good choice for b/a but then we have to decide what dimension to keep fixed. If we fix b then write

$$v = \frac{b}{a} = \cosh(\xi)$$

$$a\delta_{y_\infty} = -\frac{b}{v}\left(v^2-1\right)^{\frac{1}{2}}\left[\frac{1}{\pi}\,\text{arccosh}(v)\right]^{-\frac{1}{2}}$$

$$= -b\,\tanh(\xi)\left[\frac{\pi}{\xi}\right]^{\frac{1}{2}} \qquad \text{(C.20)}$$

Differentiating with respect to ξ for an extremum at ξ_o we find

$$\sinh(2\xi_o) = 4\xi_o\ ,\ \xi_o \simeq 1.09$$

$$\frac{b}{a} \simeq 1.65$$

$$\left|a\delta_{y_\infty}\right|_{\max} \simeq 1.35\,b$$

$$f_g \simeq .347 \left(\simeq 131\ \Omega \text{ in free space}\right) \qquad \text{(C.21)}$$

This is only illustrative since other parameters (e.g. b+a) could be kept fired, giving a different optimum.

4. S_a with hyperbolic boundary

Now we need not integrate over all S but restrict S_a to something more practical. Noting that S_a can be chosen as the aperture for a long TEM horn, parts of S can be covered with a conductor to remove tangential electric field with a component opposite to that of the principal field. For use with a reflector the metal includes portions of S with components in the principal field direction, i.e. in the -y direction.

As discussed in Section II for x, z and y, z symmetry planes for S_a we have

$$h_{a_y} = \frac{4}{\Delta v}\int_0^{x\max} u_a dx = \frac{2}{\pi}\int_0^{x\max} u_a dx_a \qquad \text{(C.22)}$$

where u_a is the electric potential along the upper edge of S_a'. So let us find $u_a\,(x_a)$ such that it is maximized for each x_a at a position y_a. Differentiating u in (C.3) with respect to y and setting to zero for an extremum gives the C_a contour as

$$\left(\frac{y_a}{b_e}\right)^2 = 1 + \left(\frac{x_a}{b_e}\right)^2 \qquad \text{(C.23)}$$

which is a hyperbola, applying outside the conductors. Note in limiting cases (first quadrant)

$$\frac{y_a}{b_e} \rightarrow \begin{cases} 1 \text{ for small } \dfrac{x_a}{b_e} \\ \dfrac{x_a}{b_e} \text{ for large } \dfrac{x_a}{b_e} \end{cases} \qquad \text{(C.24)}$$

If we extend this shape of S_a to ∞ it occupies one half of S_∞ as $\Psi_\infty \rightarrow \infty$. Note that a small region is excluded (circular of radius a centered on $y=b$). Note also that this contour can be found on fig. C.1 by considering each contour of constant u and finding its right most extremum (i.e. maximum value achieved by x/b_e for all y/b_e).

Noting that the contour meets the conductor at

$$\zeta_a = x_a + jy_a = a + jb$$

$$u_a = u_+ \qquad \text{(C.25)}$$

then (C.22) becomes

$$h_{a_y} = \frac{2}{\pi}\left\{ au_+ + \int_a^{x_{max}} u_a dx_a \right\}$$

$$= \frac{2}{\pi}\left\{ au_+ + \frac{b_e}{2}\int_{\psi_o}^{\psi_{max}} \ell n \left[\frac{\psi^2 + \left[1+\left[1+\psi^2\right]^{\frac{1}{2}}\right]^2}{\psi^2 + \left[1-\left[1+\psi^2\right]^{\frac{1}{2}}\right]^2} \right] d\psi \right\}$$

$$= \frac{2}{\pi}\left\{ au_+ + \frac{b_e}{2}\int_{\psi_o}^{\psi_{max}} \ell n \left[\frac{\left[1+\psi^2\right]^{\frac{1}{2}}+1}{\left[1+\psi^2\right]^{\frac{1}{2}}-1} \right] d\psi \right\}$$

$$= \frac{2}{\pi}\left\{ au_+ + b_e\int_{\psi_o}^{\psi_{max}} \text{arccsch}(\psi) d\psi \right\}$$

$$\psi \equiv \frac{x_a}{b_e}, \quad \psi_o \equiv \frac{a}{b_e}, \quad \psi_{max} \equiv \frac{x_{max}}{b_e} \qquad \text{(C.26)}$$

Using standard tables [8, 9] we have

$$h_{a_y} = \frac{2}{\pi}\left\{ au_+ + b_e\left[\psi \operatorname{arccsch}(\psi)\right]\Big|_{\psi_o}^{\psi_{max}} \right\}$$

$$= \frac{2}{\pi}\left\{ au_+ + b_e \left[\psi_{max}\operatorname{arccsch}(\psi_{max}) + \operatorname{arcsinh}(\psi_{max}) \right.\right.$$

$$\left.\left. -\psi_o \operatorname{arccsch}(\psi_o) - \operatorname{arcsinh}(\psi_o)\right]\right\} \qquad \text{(C.27)}$$

For small a/b we have

$$au_+ \to 0 \ , \ \psi_o \to 0 \ , \ x_o \to 0$$

$$\operatorname{arcsinh}(\psi_o) = \psi_o + 0\left(\psi_o^3\right)$$

$$\psi_o \operatorname{arccsch}(\psi_o) = \psi_o \ell n\left(\frac{2}{\psi_o}\right) + 0\left(\psi_o^3\right) \qquad \text{(C.28)}$$

giving

$$h_{a_y} = b_e \frac{2}{\pi}\left\{\psi_{max}\operatorname{arccsch}(\psi_{max}) + \operatorname{arcsinh}(\psi_{max})\right\}$$

$$\text{as } x_o \to 0 \qquad \text{(C.29)}$$

Now consider how large one may wish to make such a reflector. For large x_{max} we have

$$x_{max} \to \infty \quad , \quad \psi_{max} \to \infty$$

$$\operatorname{arcsinh}(\psi_{max}) = \ell n(2\psi_{max}) + 0\left(\psi_{max}^{-2}\right)$$

$$\psi_{max}\operatorname{arccsch}(\psi_{max}) = 1 + 0\left(\psi_{max}^{-2}\right) \qquad \text{(C.30)}$$

giving (for negligible x_o)

$$h_{a_y} = \frac{2}{\pi}\left\{1 + \ell n(2\psi_{max}) + 0\left(\psi_{max}^{-2}\right)\right\}$$

$$= \frac{2}{\pi} b_e \left\{1 + \ell n\left(\frac{2x_{max}}{b_e}\right) + 0\left(x_{max}^{-2}\right)\right\}$$

$$\text{as } x_{max} \to \infty \qquad \text{(C.31)}$$

The point is that this diverges, so h_{a_y} can be made (in principle) as large as one wishes by appropriate choice of x_{max}.

In practice as x_{max} is made larger and larger the structure is inefficient in that b_e could be made larger instead, h_{a_y} being first order in b_e instead of only logarithmic in x_{max} (for large x_{max}/b_e). In addition the largest radius of S_a determines the required length of a conical transmission line and/or size of lens or reflector to produce an acceptable wave planarity (simutaneity of arrival) over the aperture.

5. Rectangular aperture

Another shape we can consider is a rectangle with boundaries

$$x = \pm x_{max} \quad , \quad y = \pm b_e \tag{C.32}$$

Then we have the x coordinate as x_o where the contour meets the conductor in the first quadrant as

$$\psi_o = \frac{x_o}{b_e} \quad , \quad v = \frac{b}{a}$$

$$u_+ = \text{arccosh}(v) = \ell n\left[v + \left(v^2 - 1\right)^{\frac{1}{2}}\right]$$

$$= \frac{1}{2}\,\ell n\left[1 + 4\psi_o^{-2}\right]$$

$$\psi_o = 2\left\{\left[v + \left(v^2 - 1\right)^{\frac{1}{2}}\right]^2 - 1\right\}^{-\frac{1}{2}}$$

$$= \sqrt{2}\left(v^2 - 1\right)^{-\frac{1}{2}}\left[v + \left(v^2 - 1\right)^{\frac{1}{2}}\right]^{-\frac{1}{2}}$$

$$= \sqrt{2}\left(\frac{b_e}{a}\right)^{-\frac{1}{2}}\left[\frac{b + b_e}{a}\right]^{-\frac{1}{2}}$$

$$\rightarrow \frac{a}{b_e} = v^{-1} \text{ for small } \frac{a}{b} \text{ (large } v\text{)} \tag{C.33}$$

From (C.22) we then have

$$h_{a_y} = \frac{2}{\pi}\left\{x_o u_+ + \int_{x_o}^{x_{max}} u_a \, dx_a\right\}$$

$$= \frac{2}{\pi}\left\{x_o u_+ + \int_{\xi_1}^{\xi_o} \xi^{-2} \, \ell n\left[1 + \xi^2\right] \, d\xi\right\}$$

$$\xi \equiv 2\frac{b_e}{x_a} \, , \; \xi_o \equiv 2\frac{b_e}{x_o} \, , \; \xi_1 \equiv 2\frac{b_e}{x_{max}} \qquad \text{(C.34)}$$

Integrating by parts gives

$$h_{a_y} = \frac{2}{\pi}\left\{x_o u_+ - b_e \xi^{-1} \ell n\left[1+\xi^2\right]\Big|_{\xi_1}^{\xi_o} + 2b_e \int_{\xi_1}^{\xi_o}\left[1 + \xi^2\right]^{-1} d\xi\right\}$$

$$= \frac{2}{\pi} x_o u_+ - \frac{2}{\pi} b_e \left\{\frac{\ell n\left[1+\xi_1^2\right]}{\xi_1} - \frac{\ell n\left[1+\xi_0^2\right]}{\xi_o}\right.$$

$$\left. + \; 2 \arctan\left(\xi_o\right) - 2\arctan\left(\xi_1\right)\right\} \qquad \text{(C.35)}$$

For small x_o we have

$$\xi_o \to \infty$$

$$h_{a_y} = b_e \frac{2}{\pi}\left\{\frac{\ell n\left[1 + \xi_1^2\right]}{\xi_1} + \pi - 2 \arctan(\xi_1)\right\}$$

$$\text{as } x_o \to 0 \qquad \text{(C.36)}$$

Now look at how wide one may wish to make the rectangular reflector. One can make it infinitely wide in which case

$$\xi_1 \to 0+$$

$$h_{a_y} = 2b_e = h_{e_y} \quad \text{as } x_o \to 0$$

$$x_{max} \to \infty \qquad \text{(C.37)}$$

Again we get back to the equivalent height.

A special case of a rectangle is a square for which

$$x_{\max} = b_e \quad , \quad \xi_1 = 2$$

$$h_{a_y} = b_e\left\{2 + \frac{\ell n(5)}{\pi} - \frac{4}{\pi}\arctan(2)\right\} \text{ as } x_o \to 0$$

$$\simeq 1.10\ b_e \tag{C.38}$$

which is slightly more than for the circular aperture in (C.17).

Appendix D. Surface Integral over All S in Terms of Equivalent Height

Using the transformation in Appendix C for two wires, let us extend the results to more general cases. Consider the quantity

$$b_y \equiv \frac{2}{\pi} \oint_{C'_a} v dy \tag{D.1}$$

in the limit as the radius of the wire goes to zero. With C'_a around the first quadrant of the ζ plane we find that

$$b_y = 2b_e \tag{D.2}$$

as in (C.15) with $v_o = 0$. This is just the separation between the two line charges, or the equivalent height. Note that this applies when S_a is extended to the entire plane S, but in a limiting sense where $v_o \to 0$. Since the lines of constant v are circles described by (C.13), extending in the first quadrant approximately twice as far in the $+x$ direction (for small v_o) as in the $+y$ direction, the result applies for such an aperture shape, and may not give the same result as for a large circular aperture (to be discussed later).

Generalizing this, note that in complex form the effective length of the aperture is

$$a_\delta = -[\Delta u \, \Delta v]^{-1/2} W_a = -f_g^{-1/2} \frac{W_a}{\Delta v}$$

$$W_a = j \oint_{C_a} u d\zeta^* = -\oint_{C_a} v d\zeta^* \tag{D.3}$$

Rearrange this for the case that S_a is extended to the entire plane S as

$$h_e \equiv f_g^{1/2} a_\delta = -\frac{W_v}{\Delta v}$$

$$= h_{e_x} - j h_{e_y} \tag{D.4}$$

where W_v indicates the sense of the limit as $v_o \to 0$. In Appendix C this takes special forms due to the symmetry of the particular problem and the fact that Δv is 2π. Here we have using the general forms in Appendix B

$$h_e = -\frac{W_v}{\Delta v} = -\frac{1}{\Delta v} \int_{S_v} \frac{dw(\zeta)}{d\zeta} dxdy$$

$$= -\frac{j}{\Delta v} \oint_{C_v} u d\zeta^* = \frac{1}{\Delta v} \oint_{C_v} v d\zeta^* \tag{D.5}$$

where C_v is now interpreted as a contour with $v_o \to 0$ with appropriate deformation as in Appendix B to avoid branch cuts. Furthermore this contour has to be aligned according to the orientation of h_e.

Now we can think of generalizing this result to arbitrary shapes of the two conductors (+ and -) in fig. A.1. Essentially we move the line charge around the surface of the conductor, weight h_e by the local

charge density on the conductor, and integrate over the conductors. This makes h_e the average charge separation distance, the equivalent height for the more general case. This is just a superposition result regarding the integral of the fields over S_v as the sum of integrals for each part of the surface charge distribution.

An alternate approach to this integral and its relation to h_e is found by considering a circular aperture of radius Ψ_∞ and let $\Psi_\infty \to \infty$. For this purpose let us use the electric - potential form and evaluate

$$a_g f_g^{1/2} = -\frac{W_\infty}{\Delta v} = -\frac{1}{\Delta v}\oint_{S_\infty} \frac{dw(\zeta)}{d\zeta}\, dxdy$$

$$= -\frac{j}{\Delta v}\oint_{C_\infty} u d\zeta^* = \frac{1}{\Delta v}\oint_{C_\infty} v d\zeta^* \qquad \text{(D.6)}$$

where C_∞ a circle of radius $\Psi_\infty \to \infty$ with deformation as in fig. A.1 to avoid branch cuts.

Consider the contribution from the contour C_o in fig. A.1. Note that inside C_o the electric fields are zero (inside the conductors) or cover zero area (between C_r and C_ℓ). On the conductors the electric potential is constant so we have (from (B.11))

$$\oint_{C_+} u_+ d\zeta^* = 0 = \oint_{C_-} u_- d\zeta^* \qquad \text{(D.7)}$$

The electric potential is continuous across the branch cut so we have

$$\oint_{C_+} u d\zeta^* + \oint_{C_-} u d\zeta^* = 0 \qquad \text{(D.8)}$$

So for the contribution from C_o we have

$$W_o = j\oint_{C_o} u d\zeta^* = 0 \qquad \text{(D.9)}$$

and we have for the entire plane

$$W_\infty = j\oint_{C_\infty} u d\zeta^* \qquad \text{(D.10)}$$

where now C_∞ is just the circle of radius C_∞, this result applying to the electric potential.

So now we need the asymptotic behavior of u for large $|\zeta|$. In terms of the electric potential we have in cylindrical coordinates [10]

$$x = \Psi\cos(\phi)\ ,\ y = \Psi\sin(\phi)$$

$$\Phi = [a_o\phi + b_o][c_o\ell n(\Psi) + d_o]$$

$$+ \sum_{n=1}^{\infty}\Big[a_n\cos(n\phi) + b_n\sin(n\phi)\Big]\Big[c_n\Psi^n + d_n\Psi_n^{-n}\Big] \tag{D.11}$$

Reject the $\ell n(\Psi)$ term as applying to non-zero net charge per unit length and the ϕ term as applying to the corresponding Φ_m for non-zero net current. Reject the Ψ^n terms since there is no charge at ∞. This leaves the form

$$\Phi = b_o + \sum_{n=1}^{\infty}\Big[a_n\cos(n\phi) + b_n\sin(n\phi)\Big]\Psi_n^{-n} \tag{D.12}$$

with remaining acceptable terms.

Write (D.10) in terms of Φ as

$$W_\infty = \lim_{\Psi_\infty\to\infty} j\oint_{C_\infty} ud\zeta^* = \lim_{\Psi_\infty\to\infty} j\frac{\Delta u}{V}\oint_{C_\infty}\Phi d\zeta^* \tag{D.13}$$

Apply this to each term in (D.12). By (B.11) the constant term gives zero. So do all terms with $n \geq 2$, being $0\left(\Psi_\infty^{-n+1}\right)$. Thus we have

$$W_\infty = \lim_{\Psi_\infty\to\infty} j\frac{\Delta u}{V}\int_0^{2\pi}[a_1\cos(\phi) + b_1\sin(\phi)]\frac{d\zeta^*}{\Psi_\infty}$$

$$= j\frac{\Delta u}{V}\int_0^{2\pi}[a_1\cos(\phi) + b_1\sin(\phi)]\ [d(\cos(\phi)) - jd(\sin(\phi))]$$

$$= j\frac{\Delta u}{V}\int_0^{2\pi}[a_1\cos(\phi) + b_1\sin(\phi)]\ [-\sin(\phi) - j\cos(\phi)]d\phi$$

$$= \frac{\Delta u}{V}\ \pi\ [a_1 - jb_1] \tag{D.14}$$

Consider a line dipole of strength

$$\vec{p}' = q'\ \vec{h}_e \tag{D.15}$$

As indicated in fig. A.1 the equivalent height $\vec{h}_e$ measures the mean charge separation distance on the conductors and is illustrated here oriented in the y direction. The potential for such a dipole in the limit of small $\vec{h}_e$ with

$$\vec{p}' = p'_y \, \vec{1}_y \tag{D.16}$$

can be evaluated as the potential of two closely spaced, oppositely charged, line charges. From Appendix C we have for two line charges of $\pm q'$ spaced $\pm h_y / 2$ along the y axis

$$\Phi = \frac{V}{\Delta u} u = \frac{q'}{C'} \frac{u}{\Delta u} = \frac{q'}{C' f_g} \frac{u}{\Delta v} = \frac{q'}{\epsilon_o} \frac{u}{\Delta v}$$

$$w = \ell n \left[\frac{\frac{2\zeta}{h_y} + j}{\frac{2\zeta}{h_y} - j} \right]$$

$$\Delta v = 2\pi \tag{D.17}$$

Expanding the potential for large $|\zeta|$ we have

$$w = \ell n \left[\frac{1 + \frac{j h_y}{2\zeta}}{1 - \frac{j h_y}{2\zeta}} \right] = j \frac{h_y}{\zeta} + 0\left(\left(\frac{h_e}{\zeta} \right)^2 \right)$$

$$u = \frac{h_y \; y}{\Psi^2} + 0\left(\left(\frac{h_y}{\Psi} \right)^2 \right) = \frac{h_y \sin(\phi)}{\Psi} + 0\left(\left(\frac{h_e}{\Psi} \right)^2 \right) \tag{D.18}$$

This gives an electric potential

$$\Phi = \frac{p'_y}{2\pi \epsilon_o} \left[\frac{\sin(\phi)}{\Psi} + 0\left(\frac{h_e}{\Psi^2} \right) \right] \tag{D.19}$$

and we can let $h_y \to 0$ for a simple form of the potential. As one should expect the potential at large Ψ is dominated (for zero net charge) by the line dipole moment.

Comparing this potential to that in (D.12) observe that

$$b_1 = \frac{p'_y}{2\pi \epsilon_o} \, , \; W_\infty = -j \frac{\Delta u}{V} \frac{p'_y}{2\epsilon_o} \tag{D.20}$$

Similarly choosing an x directed line dipole of strength p'_x replaces $\sin(\phi)$ by $\cos(\phi)$ in (D.19) giving

$$a_1 = \frac{p'_x}{2\pi \epsilon_o} \, , \; W_\infty = -j \frac{\Delta u}{V} \frac{p'_x}{2\epsilon_o} \tag{D.21}$$

Combining these gives

$$\vec{p}' = \vec{p}'_x \vec{1}_x + p'_y \vec{1}_y = q' h_e$$

$$\vec{h}_e = h_x \vec{1}_x + h_y \vec{1}_y$$

$$p' = p'_x - jp'_y = q' h_e$$

$$h_e = h_x - jh_y \tag{D.22}$$

Then we have

$$W_\infty = \frac{\Delta u}{V} \frac{p'}{2\epsilon_o} = \frac{\Delta u}{V} \frac{q' h_e}{2\epsilon_o} = \Delta u \frac{C' h_e}{2\epsilon_o}$$

$$= \frac{\Delta u}{f_g} \frac{h_e}{2} = \frac{\Delta v}{2} h_e \tag{D.23}$$

While the particular transformation (D.17) has a Δv of 2π, the result is cast in the form of a general Δv for greater generality.

Comparing to (A.4) we now have

$$a_\delta = -f_g^{-\frac{1}{2}} \frac{W_\infty}{\Delta v} = -f_g^{-\frac{1}{2}} \frac{h_e}{2} \tag{D.24}$$

i.e., a factor of two smaller result. So for a circular S_a with $\Psi_\infty \to \infty$ the result is reduced by half from that for the special aperture shape S_v based on constant v contours. The result for an infinite aperture then depends on the way the limit to ∞ is taken. In integral form we also have

$$h_e = 2\frac{W_\infty}{\Delta v} = -2 f_g^{1/2} a_\delta$$

$$= j\frac{2}{\Delta v} \oint_{C_\infty} u d\zeta^* \tag{D.25}$$

This can be put in terms of the magnetic potential also if we include the C_o contribution.

The result for an infinite circular aperture is an appropriate one to use because it models a practical physical situation. Consider that the aperture illumination comes from some finite source, such as a conical transmission line of finite length. This means that the entire aperture plane cannot be simultaneously filled with electric field. The finite propagation speed of light c means that signals from the conical apex (launch point) arrive on S, filling out a circular portion with radius expanding as time increases. For a given circle the fill time (from first to last arrival) can be made arbitrarily short if the length of the conical launcher (in the z direction) is made sufficiently large.

References

1. C. E. Baum, Impedances and Field Distributions for Symmetrical Two Wire and Four Wire Transmission Line Simulators, Sensor and Simulation Note 27, October 1966.

2. C. E. Baum, The Conical Transmission Line as a Wave Launcher and Terminator for a Cylindrical Transmission Line, Sensor and Simulation Note 31, January 197.

3. C. E. Baum, D. V. Giri, and R. D. Gonzales, Electromagnetic Field Distribution of the TEM Mode in a Symmetrical Two-Parallel-Plate Transmission Line, Sensor and Simulation Note 219, April 1976.

4. C. E. Baum, Radiation of Impulse-Like Transient Fields, Sensor and Simulation Note 321, November 1989.

5. C. E. Baum, Configurations of TEM Feed for an IRA, Sensor and Simulation Note 327, April 1991.

6. M. Kanda, Transients in a Resistively Loaded Linear Antenna Compared with Those in a Conical Antenna and a TEM Horn, IEEE Trans. Antennas and Propagation, 1980, pp. 132-136.

7. R. V. Churchill, Complex Variables and Applications, McGraw Hill, 1960.

8. H. B. Dwight, Tables of Integrals and Other Mathematical Data, 4th Ed., Macmillan, 1961.

9. M. Abramowitz and I. A. Stegun, Handbook of Mathematical Functions, AMS 55, U. S. Gov't Printing Office, 1964.

10. W. R. Smythe, Static and Dynamic Electricity, 3rd Ed., McGraw Hill, 1968 (reissued 1989, Hemisphere Publishing Corp.).

11. T. M. Apostol, Calculus, 2nd Ed., Vol. II, Blaisdell, 1969.

12. C. E. Baum and A. P. Stone, Transient Lens Synthesis: Differential Geometry in Electromagnetic Theory, Hemisphere Publishing Corp., 1991.